

Macroscopic phase separation of Se-rich ($x < 1/3$) ternary $\text{Ag}_y(\text{Ge}_x\text{Se}_{1-x})_{1-y}$ glasses

Y Wang¹, M Mitkova^{1,2}, D G Georgiev¹, S Mamedov¹ and P Boolchand¹

¹ Department of ECECS, University of Cincinnati, Cincinnati, OH 45221-0030, USA

² Center for Solid State Electronics Research, Arizona State University, Tempe, AZ 85287-6206, USA

Received 13 November 2002

Published 14 April 2003

Online at stacks.iop.org/JPhysCM/15/S1573

Abstract

Temperature modulated differential scanning calorimetry measurements on $\text{Ag}_y(\text{Ge}_x\text{Se}_{1-x})_{1-y}$ glasses provide evidence for bimodal glass transition temperatures in Se-rich glasses ($x < 1/3$). At $x = 0.20$ and 0.25 , thermal measurements performed as a function of Ag content in the $0 \leq y \leq 0.25$ range reveal that the additive (Ag) segregates into an Ag_2Se -rich *glass phase*, possessing a characteristic glass transition temperature $T_g^a = 230^\circ\text{C}$, while the *remaining base glass* displays a second glass transition temperature T_g^b that systematically increases as its Se content is depleted. The present thermal results are in harmony with Raman scattering, neutron diffraction, dielectric spectroscopy and optical microscopy measurements and suggest that Se-rich glasses in the Ag–Ge–Se ternary system intrinsically phase separate on a macroscopic scale.

1. Introduction

Ag-containing chalcogenide glasses have attracted widespread interest for applications in optical recording [1] and as solid electrolytes [2]. While most of this work has been performed on amorphous Ge–Se thin films in which Ag has been photo-diffused [3], important insight into the physical behaviour of these films has emerged by examining the corresponding bulk glasses. The experimental methods used include neutron diffraction [4], Raman scattering [5], differential scanning calorimetry (DSC) [4], electrical conductivity [6], dielectric spectroscopy [7] and optical microscopy [7]. In spite of this large database, there continues to be a debate on basic aspects of the glass structure. For example, neutron diffraction [4], vibrational spectroscopy [5] and DSC [5] results on the ternary $\text{Ag}_y(\text{Ge}_x\text{Se}_{1-x})_{1-y}$ glass with composition $x = y = 1/4$ were found to be consistent with a *homogeneous* network structure. This view is, however, in sharp contrast to a molecular dynamics study [8] on the same glass [5] which suggests that Ag is clustered.

Diffraction methods [8–12] have traditionally served as a direct means of probing liquid and glass structure, although analyses of structure factors have required increasingly

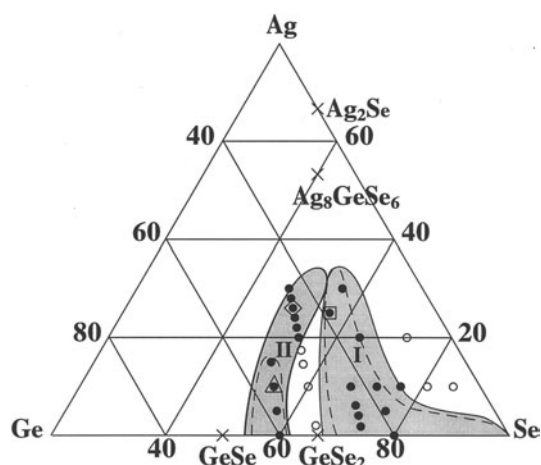


Figure 1. Glass-forming regions in the Ag–Ge–Se ternary system taken from [19]. The Se-rich and Ge-rich regions are denoted by I and II respectively.

sophisticated theoretical models [8–10]. Even with the most recent *ab initio* molecular dynamics procedures [9, 10], artifacts of chemical disorder invariably appear to be frozen in because of the rapid quench rates used (or short simulation times employed) to synthesize glasses in these numerical experiments. Existing computational capabilities do not permit a relaxation of computer synthesized networks for periods much longer than a nanosecond, which is significantly shorter than the timescale (of a few seconds) typical of atomic scale structural relaxation in the laboratory near the glass transition temperature T_g . Fortunately, crucial insight into glass structure, at both a local and medium-range level, can be independently accessed by local probes (e.g. nuclear quadrupole resonance, nuclear magnetic resonance, Mössbauer effect) [13, 14], by vibrational spectroscopies (e.g. IR and Raman scattering) [15] and, in particular, by thermal analysis methods. Glass transition temperatures provide a global measure of network connectivity as elegantly demonstrated by stochastic agglomeration theory in a series of publications by Kerner and Micoulaut [16, 17]. Experimentally, the recently introduced T -modulated variant of differential scanning calorimetry (MDSC), in contrast to DSC, offers the prospect of not only a higher sensitivity for the measurement of T_g values but also a means for establishing these characteristic temperatures independent largely of scan rate and thermal history effects [18].

In this communication we report on the molecular structure of bulk quenched $\text{Ag}_y(\text{Ge}_x\text{Se}_{1-x})_{1-y}$ glasses at $x = 0.20$ and 0.25 as a function of Ag additive concentration in the $0 \leq y \leq 0.25$ range. These glasses form part of the Se-rich compositions [19] (region I) in the Ag–Ge–Se ternary system (figure 1) where apparently the glass-forming tendency is optimized. We have examined these compositions in MDSC experiments. An analysis of the results by using constraint counting algorithms [20–23], along with the information provided by vibrational spectroscopy [19], neutron diffraction [5, 8], dielectric spectroscopy [7] and optical microscopy methods [7], shows that glasses in region I are *intrinsically phase separated* [19] on a macroscopic scale. In sharp contrast, Ge-rich glasses ($x > 1/3$, region II in figure 1), separated from region I by a corridor, display single T_g values and the Ag forms part of the base-glass network [19]. These latter compositions will not be discussed in the present work.

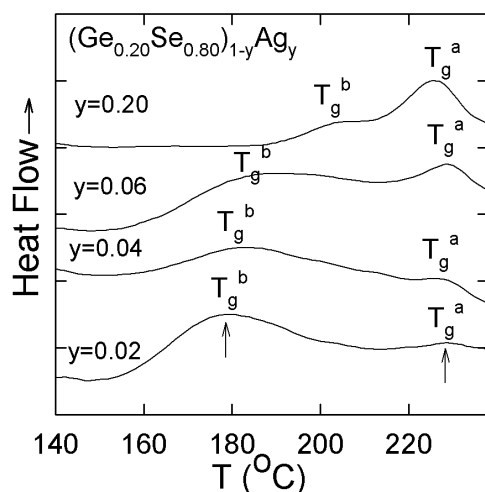


Figure 2. Total heat flow in MDSC scans of $\text{Ag}_y(\text{Ge}_{0.20}\text{Se}_{0.80})_{1-y}$ glasses with increasing Ag content showing the evolution of bimodal T_g values. In these scans the low- T endotherm is identified with the base glass (T_g^b) while the high- T endotherm is identified with the additive Ag_2Se glass phase (T_g^a)—see the text for details.

2. Experimental results

The bulk glasses were prepared [19] by reacting 99.999% Ge, Se and Ag in evacuated quartz tubes (5 mm inner diameter, 1 mm wall thickness) at 950 °C for several days by periodic shaking. Melts were equilibrated at 830 °C and then water quenched. MDSC scans of the samples were taken at a 3 °C min⁻¹ scan rate and a 1 °C 100 s⁻¹ modulation rate using a model 2920 TA Instruments unit. In MDSC, glass transition temperatures are deduced from the inflection point of the reversing heat flow [15] and a typical measurement error is ± 1 °C.

Figure 2 displays the total heat flow in MDSC scans of $\text{Ag}_y(\text{Ge}_{0.20}\text{Se}_{0.80})_{1-y}$ glasses at several Ag concentrations in the $0 \leq y \leq 0.20$ range. One can discern two endotherms, a low- T one centred near 180 °C that systematically shifts up in T and decreases in strength (or step-size ΔC_p in the constant pressure heat capacity) as a function of increasing Ag concentration, and a second, high- T , one centred near 230 °C that does not shift with Ag concentration but which progressively increases in strength. As discussed later, in these scans the endotherm that shifts up with Ag content will be identified with the glass transition temperature of the base glass and will henceforth be labelled $T_g^{\text{base}} = T_g^b$, while the endotherm that does not shift with Ag content is identified with that of the additive-rich Ag_2Se glass phase and is labelled as $T_g^{\text{additive}} = T_g^a$.

Figure 3(a) shows MDSC scans of an $\text{Ag}_y(\text{Ge}_{0.25}\text{Se}_{0.75})_{1-y}$ sample at $y = 0.20$. Two glass transitions are again observed, one at $T_g^a = 240$ °C and a second one, T_g^b , near 281 °C. In MDSC, the reversing heat flow signal always sits on a flat baseline, regardless of the equipment baseline. Indeed, if only a single T_g were associated with the scan of figure 3(a), one would have expected the reversing heat flow to level off as shown by the broken curve. Note that use of a larger Ge concentration ($x = 0.25$) for the base glass in relation to the previous sample ($x = 0.20$; results of figure 2) reverses the order of T_g^a and T_g^b . In figure 3(a), we observe the first crystallization exotherm, $T_x^1 = 302$ °C. By partially crystallizing the virgin glass at T_x^1 for several minutes, we are able to partially suppress the first glass transition endotherm at T_g^a , as can

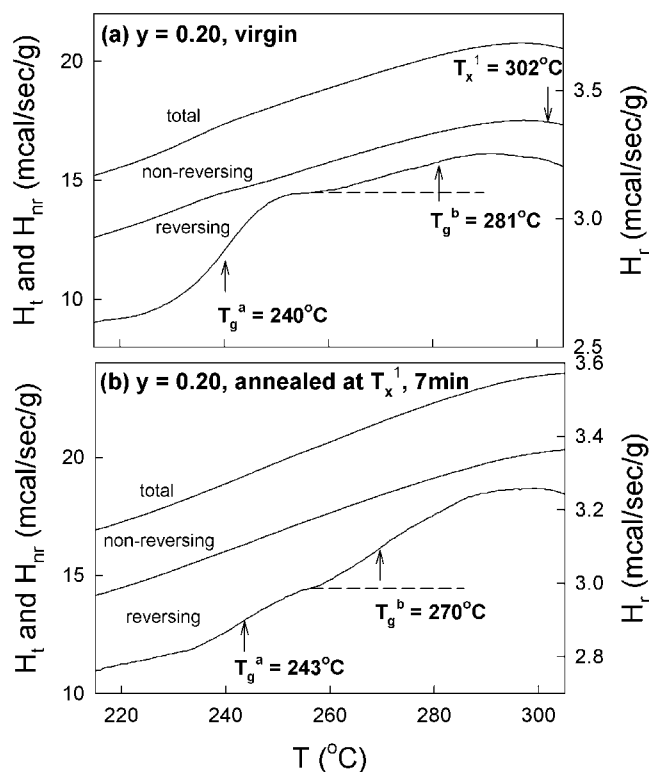


Figure 3. MDSC scans of an $\text{Ag}_y(\text{Ge}_{0.25}\text{Se}_{0.75})_{1-y}$ glass at $y = 0.20$ in the (a) virgin and (b) partially crystallized state. Upon heating at the indicated crystallization temperature T_x^1 , the low- T_g^a endotherm is suppressed and the high- T_g^b endotherm is enhanced. The sizes of the reversing heat flow steps for the 'a' (additive) and 'b' (base) glass phases are related to the contents of these phases in the glass of interest.

be seen in figure 3(b), and one now observes the second (T_g^b) endotherm to increase in strength and also to move to a slightly lower temperature of 270 °C. These results suggest that phases giving rise to processes at T_g^a and T_x^1 are generically related, a point to which we will later return.

Figure 4(a) shows MDSC results for a $\text{Ag}_{0.25}(\text{Ge}_{0.25}\text{Se}_{0.75})_{0.75}$ glass sample in which a glass transition is observed near $T_g^a = 230$ °C and a crystallization exotherm onset near $T_x^1 = 295$ °C. Figure 4(b) shows a scan of the same sample after it has been partially crystallized by heating at T_x^1 for 6 min, and now we observe a second glass transition at $T_g^b = 290$ °C. One can observe the T_g^b endotherm largely because the large exotherm at T_x^1 has been removed by crystallizing the relevant (additive) phase. Thus we observe two distinct glass transitions (T_g^a, T_g^b) at $y = 1/4$, except the glass transition T_g^b is now shifted up in temperature by comparison with T_g^b for $y = 0.20$.

Figure 5 provides a summary of the compositional trends of the bimodal glass transition temperatures (T_g^a, T_g^b) for glasses having a fixed value of $x = 1/4$, but varying concentrations (y) of Ag. With increasing y , one finds that T_g^b systematically shifts up from 230 to 290 °C, a pattern also noted at $x = 0.20$ (figure 2). Furthermore, for $y > 0.10$ the glass transition temperature, T_g^a , becomes clearly discernible and remains independent of y over the range examined. These compositional trends in T_g provide the basis for a discussion of the underlying phase transformations (section 3).

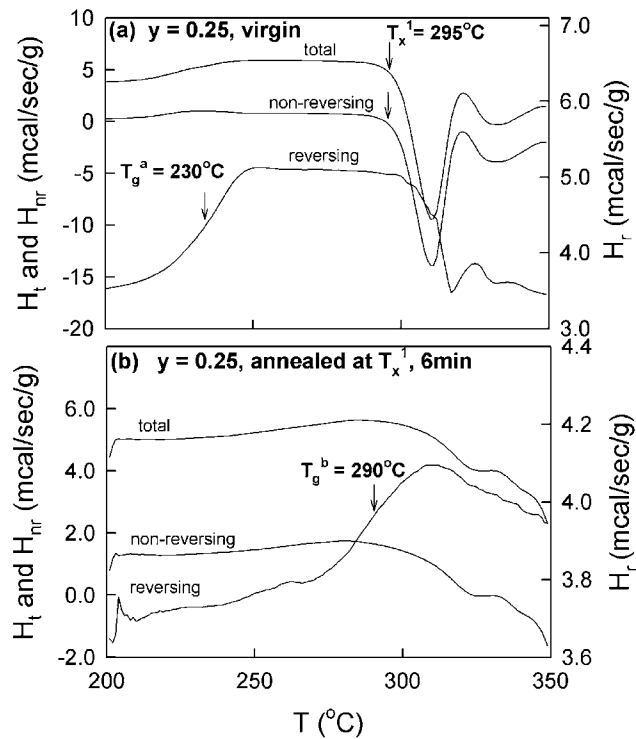


Figure 4. MDSC scans of an $\text{Ag}_y(\text{Ge}_{0.25}\text{Se}_{0.75})_{1-y}$ glass at $y = 0.25$ in the (a) virgin and (b) partially crystallized state. The T_g^a ($=230^\circ\text{C}$) endotherm is observed in the virgin sample, while the T_g^b ($=290^\circ\text{C}$) endotherm is observed in the partially crystallized sample.

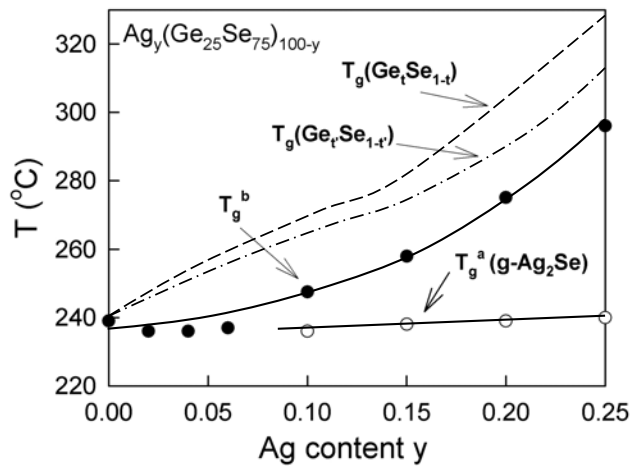


Figure 5. Evolution of bimodal glass transition temperatures (T_g^a , T_g^b) upon increasing the Ag content in $\text{Ag}_y(\text{Ge}_{0.25}\text{Se}_{0.75})_{1-y}$ glasses. The broken curve gives the anticipated behaviour of T_g^b if equation (1) is used to describe phase separation of the ternary glasses. The dot-dashed curve gives the $T_g^b(y)$ dependence as predicted by equation (4).

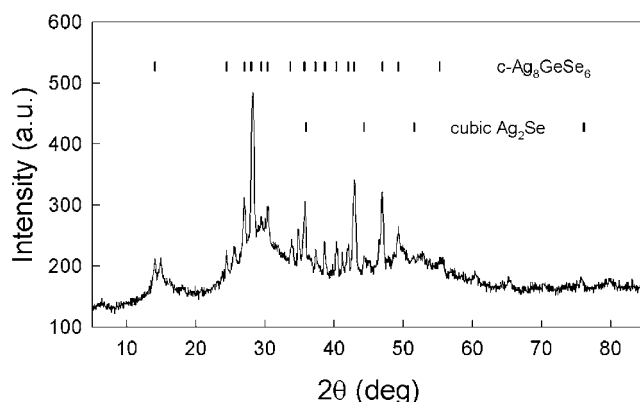


Figure 6. Powder x-ray diffraction scan of a partially crystallized $\text{Ag}_y(\text{Ge}_{0.25}\text{Se}_{0.75})_{1-y}$ glass at $y = 0.25$, heated to $T_x^1 = 295^\circ\text{C}$ for 6 min. The scattering angle is denoted by 2θ .

Powder x-ray diffraction measurements (using the Cu $K\alpha$ line with $\lambda = 1.54 \text{ \AA}$) of a glass sample at $x = y = 1/4$ heated to T_x^1 for several minutes are reproduced in figure 6. The observed reflections can be indexed after crystalline Ag_8GeSe_6 [24]. Apparently, crystallization at T_x^1 involves the Ag_2Se glass phase combining with the requisite amount of GeSe_2 (removed from the base glass) to precipitate the ternary crystal. On stoichiometric grounds, the ternary crystal ($\text{Ag}_8\text{GeSe}_6 = 4(\text{Ag}_2\text{Se}) + \text{GeSe}_2$) can be regarded as being composed of four formula units of Ag_2Se that combine with one formula unit of GeSe_2 . Thus partial crystallization of the glass by heating to T_x^1 renders the base glass slightly Ge deficient or Se rich, an idea that will enable us to provide a quantitative interpretation of the thermal results (section 3).

3. Molecular structure of Se-rich ($x < 1/3$) $\text{Ag}_y(\text{Ge}_x\text{Se}_{1-x})_{1-y}$ glasses

The foregoing thermal results can serve as the basis for an elucidation of the molecular structure of the ternary glasses, starting first with glass compositions at $x = 0.20$ and then moving on to $x = 0.25$. The deduced structures are then correlated, in sections 4 and 5, with the results obtained from other types of experiment that give information on the structure of these glasses.

3.1. Macroscopic phase separation in $\text{Ag}_y(\text{Ge}_{0.20}\text{Se}_{0.80})_{1-y}$ glasses

The MDSC results provide evidence of bimodal T_g values in *virgin* $\text{Ag}_y(\text{Ge}_{0.20}\text{Se}_{0.80})_{1-y}$ glasses. In these experiments, the low- T_g endotherm in the $180^\circ\text{C} < T_g < 200^\circ\text{C}$ range is found to systematically shift up while the second T_g appearing at a fixed temperature ($=230^\circ\text{C}$) is found to display increasingly larger ΔC_p steps with increasing Ag content.

Both these features are suggestive of a macroscopic phase separation [19] of the melts (glasses) that can be described by the following stoichiometric relationship:

$$\text{Ag}_y(\text{Ge}_x\text{Se}_{1-x})_{1-y} = (3y/2)(\text{Ag}_{2/3}\text{Se}_{1/3}) + (1 - 3y/2)\text{Ge}_t\text{Se}_{1-t}. \quad (1)$$

In equation (1), the first term on the right-hand side designates the Ag_2Se *additive glass phase* and the second term the remaining *base-glass phase*. The stoichiometry of the base glass is designated by

$$t = x(1 - y)/(1 - 3y/2). \quad (2)$$

Thus, for example, starting with a base-glass stoichiometry of $x = t = 0.20$ at $y = 0$, addition of Ag results in an increase of t to 0.24 at $y = 0.25$. It is for this reason, we believe, that the base-glass T_g^b systematically shifts up as the Ag concentration of the glasses is increased. From earlier studies [23], we know that the base-glass T_g^b equals 180 °C at $x = 0.20$ and $y = 0$, and that it is lower than T_g^a of the Ag solid-electrolyte glass phase (230 °C). Independent confirmation of this picture of macroscopic phase separation was given by alloying Ag_2Se , rather than elemental Ag, with GeSe_4 in our more recent study [25] where we found that the T_g^b shift up of the base glass is absent, thus confirming the *stoichiometry* of the additive glass phase to be close to Ag_2Se . Taken together, these thermal results are some of the first [19] to suggest that Se-rich glasses in the Ag–Ge–Se ternary system are macroscopically heterogeneous. The observation of a separate T_g^a for the additive phase in these studies suggests that the heterogeneity of the glasses occurs on a *macroscopic scale* (a few microns) and for this reason it may be seen by optical microscopy.

3.2. Macroscopic phase separation in $\text{Ag}_y(\text{Ge}_{0.25}\text{Se}_{0.75})_{1-y}$ glasses

Compositional trends in the $T_g(x)$ of binary $\text{Ge}_x\text{Se}_{1-x}$ glasses [23] reveal that as the Ge content increases from $x = 0.20$ to 0.25, T_g increases from 180 to 230 °C. This has the interesting consequence that in the ternary under study, at low Ag concentrations ($y < 0.10$), it becomes difficult to separate contributions to the glass transition endotherm of the base glass ($\text{Ge}_{0.25}\text{Se}_{0.75}$) from those of the Ag_2Se additive glass phase since their T_g values now coincide (230 °C). However, as the concentration of Ag increases further ($y > 0.15$), enough Se deficiency of the base glass sets in (equation (2)) to drive up T_g^b (base glass) so that it can be distinguished from T_g^a (Ag_2Se phase), as illustrated in figure 3(a). At still higher concentrations of Ag, such as $y = 0.25$, T_g^b shifts up to exceed T_x^1 , making it difficult to observe the T_g^b endotherm in as-quenched (virgin) samples. Upon controlled crystallization, however, it is possible to observe the glass transition of the modified base glass as shown in figures 3(b) and 4(b).

Because of its sheer simplicity, it is attractive to consider a model of glass crystallization based on equation (1). In other words, we ask the simple question: what would happen if equation (1) were also to describe partial *crystallization* of glasses upon heating to T_x^1 ? The answer is that T_g^b is expected to systematically shift up from 230 °C at $y = 0$ to 320 °C at $y = 0.25$ as shown by the broken curve in figure 5. This is the case because equation (2) fixes t , and the corresponding T_g^b values can be read off from figure 2 in [23]. Although the predicted T_g^b behaviour parallels the observed non-linear variation, it nevertheless systematically overestimates it by about 30 °C. This suggests that, although the model has the right ingredients, it is not quite complete.

As noted earlier, x-ray diffraction results reveal that the crystalline phase to nucleate at T_x^1 is $c\text{-Ag}_8\text{GeSe}_6$ (and not Ag_2Se as assumed in our simplistic model). This result suggests that the appropriate reaction to describe partial crystallization of the glass is



where the first term on the right-hand side designates the crystalline phase nucleated at T_x^1 and the second term the *remaining* base glass. The Ge stoichiometry (t') of the *remaining* base glass can be shown to be

$$t' = [x(1 - y) - y/8]/[1 - y - 7y/8]. \quad (4)$$

Equations (2) and (4) unequivocally show that $t' < t$ for a fixed value of Ag alloying y , i.e. the *remaining* base-glass Ge stoichiometry given by equation (4) is somewhat smaller than given

by equation (2). For example, for a glass with composition $x = y = 1/4$, equation (4) gives $t' = 0.29$ while equation (2) gives $t = 0.30$. The predicted T_g^b of a glass at $t = 0.30$ is 325 °C while that at $t' = 0.29$ is 315 °C, somewhat closer to the observed value (290 °C). The *remaining base glass* differs from the *virgin base glass* because crystallization of Ag_8GeSe_6 depletes some GeSe_2 from the virgin base glass, driving it somewhat Se richer and thus lowering its T_g^b . The predicted increase of $T_g^b(y)$ within such a model (shown as the dot-dashed curve in figure 5) is in better accord with the observed $T_g^b(x = 1/4, y)$ variation but the agreement is still not perfect. These results suggest that not all of the Ag additive segregates as the Ag_2Se phase but some small fraction of it alloys in the base glass to form silver thiogermanate units, $\text{Ge}(\text{Se}_{1/2})_3\text{Se}^- \text{Ag}^+$. Raman scattering evidence for such thiogermanate units has been reported in Ag–Ge–S ternary glasses [26]. The presence of such units lowers the global connectivity of the base-glass network as bridging Se sites convert to non-bridging Se^- (compensated by Ag^+ cations) to form $\text{Se}^- \text{Ag}^+$ dangling ends. Calculations show that only a few per cent (<5%) of Ag thiogermanate units would suffice to lower the global connectivity of the remaining base glass, and thus T_g^b , to account for the difference in T_g^b between the dot-dashed curve and the continuous curve of figure 5. These refinements will be discussed comprehensively in a forthcoming publication.

The results of figure 5 on these ternary glasses can thus be understood in terms of two separate glass phases present in the virgin samples: an Ag_2Se glass phase and a $\text{Ge}_t\text{Se}_{1-t}$ base-glass phase with t given by equation (2) and having a few per cent of Ag^+ dangling ends. Upon heating such a virgin glass sample to T_x^1 , the Ag_2Se glass phase in the Ge–Se base glass apparently crystallizes as Ag_8GeSe_6 , leaving behind an Se-richer base-glass phase of $\text{Ge}_{t'}\text{Se}_{1-t'}$ stoichiometry (where t' is given by equation (4)) which has a few per cent of Ag^+ dangling ends.

3.3. Homogeneous structural model of $\text{Ag}_{0.25}(\text{Ge}_{0.25}\text{Se}_{0.75})_{0.75}$ glass

The glass composition $\text{Ag}_{0.25}(\text{Ge}_{0.25}\text{Se}_{0.75})_{0.75}$ has been the subject of several earlier investigations [4, 5, 27] in which evidence for a homogeneous network description was advanced. Two previous DSC studies [5, 27] reported $T_g = 230$ °C. This observation is certainly consistent with the present work in which a T_g at that temperature is found, but is in contrast to earlier reports [5, 27] which assigned it to a homogeneous ternary glass. In the present work, as in our earlier work [19], we assign it exclusively to the additive phase (T_g^a , Ag_2Se). The base-glass transition temperature, T_g^b , somewhat exceeds T_x^1 and therefore cannot be observed in virgin samples (section 2). However, in partially crystallized samples, T_g^b is readily observed and is identified with a GeSe_2 -deficient base-glass phase. One would be hard pressed to understand the presence of a single T_g in a glass sample with $x = y = 1/4$ when two T_g values are observed at a slightly lower Ag concentration ($x = 1/4, y = 1/5$) in virgin samples as shown in figure 3(a).

The proposal in [5] of a specific 19-atom cluster of stoichiometry $\text{Ge}_3\text{Ag}_4\text{Se}_3^a\text{Se}_3^b(\text{Se}_{1/2})_6$ to account for the medium-range structure for a glass with $x = y = 1/4$ would appear to be inconsistent with the low T_g values observed. In this cluster, Ge and Ag take on coordination numbers (CNs) of four and three respectively, while Se takes on three local environments with Se^a possessing a CN = 4, Se^b a CN = 2 and six bridging Se (CN = 2) that contribute a net three atoms to the 19-atom cluster. A count of the global connectivity of this cluster yields a mean CN $\bar{r} = 3$. Structurally, the ternary Ge–Ag–Se glass system may be compared to the Ge–As–Se one, since Ag by analogy to As is thought to be threefold coordinated. If the Ge–Ag–Se glasses were to fully polymerize, as suggested in [5], one would expect a single T_g at about 450 °C. This prediction is based on a plot of $T_g(\bar{r})$ for the fully polymerized $\text{Ge}_x\text{As}_x\text{Se}_{1-2x}$ ternary [33] where the T_g values are found to increase monotonically with \bar{r} , and to acquire a value of 450 °C

near $\bar{r} = 3$. The predicted value of $T_g = 450^\circ\text{C}$ far exceeds the two T_g values of 230 and 290°C observed for the glass composition at $x = y = 1/4$. The bimodal nature of the measured T_g values and their low values suggest that the global connectivities of the two macroscopic phases are quite low ($\bar{r} < 2.5$). Furthermore, justification of a homogeneous structural model, as suggested in [5], is put into question since a molecular dynamics analysis [8] of neutron diffraction data does not support such a model.

3.4. Neutron diffraction experiments on $\text{Ag}_{0.25}(\text{Ge}_{0.25}\text{Se}_{0.75})_{0.75}$ glass

The neutron structure factor $S_n(q)$ for glassy $\text{Ag}_{0.25}(\text{Ge}_{0.25}\text{Se}_{0.75})_{0.75}$ measured by Dejus *et al* [5] has been analysed by Iyetomi *et al* [8] using molecular dynamics simulations incorporating a two-body inter-atomic potential and a system of 648 atoms, confined to a cubic box of 25.43 Å edge-length as deduced from the measured number density of the glass. In the simulations, a time step of 0.004 ps was used and the system was thermalized at 1200 K for 20 000 time steps, at 700 K for 40 000 time steps and at 300 K for 40 000 time steps, yielding a total equilibration time of 0.4 ns. In spite of the use of a short equilibration time and two-body forces, the principal features of the observed structure factor $S_n(q)$ are reproduced by the simulation [8]. The calculated pair distribution function $T(r)$ shows that the principal Ge-centred local units are $\text{Ge}(\text{Se}_{1/2})_4$ tetrahedra, in accord with Raman scattering measurements [19]. The Ag–Ag pair distribution function shows [8] a broad peak centred around 3.5 Å and Ag is thought to terminate the GeSe_2 network to form Ag_2Se -rich domains.

To decode the distribution of Ag in the simulations, the authors performed a cluster-size distribution analysis using a cut-off distance of 3.8 Å and found that the Ag atom distribution in the network is *not* random but is clustered. This broadly supports a heterogeneous structure of the glass and not a homogeneous one as was proposed by Dejus *et al* [5].

4. Dielectric spectroscopy and optical microscopy on $\text{Ag}_y(\text{Ge}_x\text{Se}_{1-x})_{1-y}$ glasses

Dielectric loss and optical microscopy measurements on Se-rich ($x = 0.25$) and Ge-rich ($x = 0.40$) glasses in the $\text{Ag}_y(\text{Ge}_x\text{Se}_{1-x})_{1-y}$ ternary system containing varying concentrations of Ag in the $0.05 < y < 0.15$ range were reported by Gutenev *et al* [7]. The dielectric loss measurements were performed using an AC bridge operating in the $10^2 < f < 10^7$ Hz frequency range. Glass samples were studied as a function of temperature $T (< T_g)$, and activation energies for carrier transport inferred from the measured relaxation times $\tau = \tau_0 \exp(E_r/kT)$. In general, plots of the dielectric loss ($\tan \delta$) displayed two peaks, a very-low-frequency one at < 1 kHz ascribed to electrical contact-related effects and a high-frequency one in the 100 kHz range related to the nature of charge carriers in the glasses. The glass-related loss peak is found to shift to lower frequencies with increasing Ag content in Se-rich as well as in Ge-rich glasses. However, the activation energies, E_r , deduced from T -dependent shifts are found to be significantly lower (0.15–0.30 eV) for the Se-rich glasses than for the Ge-rich ones (0.6–0.8 eV). The lower activation energies are attributed [7] to Ag^+ ionic conduction across *solid electrolyte inclusions in the heterogeneous Se-rich glasses*, while the higher activation energies are attributed to *electronic conduction in the homogeneous Ge-rich glasses*.

Polished slabs of the glasses were examined [7] by optical microscopy using a 400× objective. NaOH etched samples showed clear evidence of inclusions in the Se-rich glasses. The etching is known to dissolve preferentially the chalcogenide base glass thus increasing the contrast between inclusions. The size of the inclusions was found to be in the 1–3 μm range. We have performed parallel optical microscopy measurements on our Se-rich samples which confirm the existence of inclusions and their size in the micron range.

5. Intermediate phases in network glasses and Ag₂Se solid electrolyte glass phase

Pure Ag₂Se melts, upon a water quench, result in β -Ag₂Se, the non-superionic phase. A similar result is observed when Ag-containing Se melts are quenched. However, when Ag or Ag₂Se is alloyed with a Ge_xSe_{1-x} base glass in the $0.20 \leq x \leq 0.25$ range, it is possible to obtain [19] fully glassy samples containing up to 30 mol% of Ag. Base glasses at $x < 0.20$ and at $x > 0.25$ are not as conducive to glass formation with Ag, and one finds the glass-forming tendency declines slowly with Ag addition as one goes away from the privileged compositional window $0.20 \leq x \leq 0.25$. This is seen in figure 1 as a *global maximum* in the glass-forming tendency near $x = 1/4$ where glasses can be formed with rather *high Ag concentrations*.

Recent work on chalcogenide glasses has revealed [28–30] the existence of a structure-based classification into *floppy*, *intermediate* and *stressed rigid* elastic phases. Weakly cross-linked networks composed of chains of Se_n are examples of elastically *floppy* glasses. Heavily cross-linked networks, such as GeSe₂ and SiSe₂, are examples of elastically *stressed rigid* glasses. On the other hand, cross-linked networks in which the mean CN, \bar{r} , is near 2.40 represent examples of glasses in the *intermediate phase*. In the Ge_xSe_{1-x} binary system, detailed Raman scattering and MDSC results [28, 30] support the notion that glasses at $x < 0.20$ are floppy and those at $x > 0.26$ are stressed rigid, while those in the $0.20 \leq x \leq 0.26$ range belong to the *intermediate phase*. Glass compositions in the *intermediate phase* are characterized by a vanishing relaxation enthalpy (non-reversing heat flow) at T_g . This enthalpy term is generally identified with the presence of network stress in the glass.

The role of the *intermediate phase* in optimizing the glass-forming tendency of the Ag–Ge–Se system is indeed a very curious result. Glasses in the intermediate phase form networks that are *isostatically rigid* [21] i.e. networks in which the number of cross-links is just sufficient to render them rigid. *Elastically floppy* ($x < 0.20$) or *stressed rigid* ($x > 0.26$) glasses form networks that are stress prone in general [28]. The above correlation suggests that Ag₂Se inclusions in the intermediate phase are subject to no residual network stress and form glasses upon cooling because they can remain finely dispersed in the base glass. On the other hand, in stress-prone networks (floppy as well as stressed rigid compositions) we suppose that Ag₂Se fragments rapidly coalesce upon melt quenching to result in large β -Ag₂Se inclusions.

One of the recent successes of constraint-counting algorithms is that they provide important insight into the microscopic origin of glass formation of the Ag₂Se solid electrolyte phase [25]. The glass transition temperature, $T_g^a = 230$ °C, found for this phase is suggestive of a low global connectivity. The glass phase is modelled after the structure of Ag₂Se melts [30], which diffraction experiments show to be similar to that of the superionic phase α -Ag₂Se [32]. The fast-ion mobility of Ag in this phase lowers the global count of network connectedness or mean CN [25] to $\bar{r} = 2.26$ consistent with the low T_g . The calculated mean CN, $\bar{r} = 2.26$, for Ag₂Se is close to the magic value of $\bar{r} = 2.40$, the Phillips–Thorpe value. The latter is generally acknowledged [20–22] to be the critical value for optimizing the glass-forming tendency in network-forming systems. If Ag were not a highly mobile species in Ag₂Se melts, constraint-counting algorithms suggest [25] that glass formation would not be possible because of a prohibitively high global connectivity.

6. Concluding remarks

We have found evidence for bimodal glass transition temperatures in ternary Ag_y(Ge_xSe_{1-x})_{1-y} glasses for Ge in the $0.20 \leq x \leq 0.25$ concentration range and Ag in the $0 \leq y < 0.30$ concentration range, an observation which suggests that these glasses are macroscopically heterogeneous in character. At $x = 0.20$, the evolution of bimodal T_g values is observed

directly in MDSC scans (figure 2) as Ag is alloyed in the binary glass. At the higher Ge concentration of $x = 0.25$, and particularly near an Ag concentration of $y = 0.25$, the base glass T_g shifts up (305 °C) to slightly exceed the crystallization temperature, T_x^l (=290 °C), of the Ag_2Se glass phase. Detection of the base-glass T_g endotherm in the presence of the huge T_x^l exotherm is not possible, and therefore necessitates the type of partial crystallization study we have undertaken. These studies show that in the presence of a Ge–Se backbone the additive glass phase (Ag_2Se) actually crystallizes as $c\text{-Ag}_8\text{GeSe}_6$ instead of $c\text{-Ag}_2\text{Se}$. This has the related consequence that the remnant base-glass stoichiometry, after crystallization of Ag_8GeSe_6 , is slightly more Se rich than the initial glass stoichiometry. It is for this reason that the base-glass T_g values found in the *partially crystallized* samples are somewhat lower than the T_g values of the base glass in the *pristine* samples.

The picture of macroscopic phase separation suggested by the present thermal study raises the fundamental and broader issue: when does a glass network intrinsically phase separate? In general, when the global connectivity of a network, \bar{r} , exceeds 2.40 glassy networks become stressed rigid [21]. At high global connectivity, such as $\bar{r} = 3$, there will always be a tendency for melts to phase separate and lower the global connectivity by demixing: the free energy of the melts is lowered by the process of phase separation on a nanoscale [33] or, occasionally, even on a microscale as observed in the present work. In select cases, nanoscale phase separation can be delayed or even completely suppressed either by chemical disorder, as found in the Ge–As–Se ternary containing equal concentrations of Ge and As [33], or by minimizing atom size mismatch, as in the Si–Se binary [23], or even by having closely lying crystalline phases that are optimally coordinated, as in the case of the AgAsS_2 glass [25, 34]. The immiscibility of the solid electrolyte glass phase with the semiconducting base glass (in the present system) is also driven by packing considerations since the molar volumes of the former exceed those of the latter by nearly a factor of 2. For these reasons, a ternary glass at $y = 0.25$ made up of two distinct *macro*phases having $\bar{r} = 2.26$ (Ag_2Se) and $\bar{r} = 2.60$ ($\text{Ge}_{0.30}\text{Se}_{0.70}$) will certainly have a lower free energy than a homogeneous network with $\bar{r} = 3$. Careful studies on glasses have shown that the popular homogenous continuous random network description is not the rule but really an exception. A particularly interesting recent [35] exception is that of ternary Ge–S–I glasses. Here the halogen randomly cuts S bridges of the backbone, and glasses reveal a rather sharp floppy to stressed rigid transition with little or no intermediate phase.

Acknowledgments

We acknowledge discussions with M Kozicki, A Pradel and P Vashishta during the course of this work. This work is supported by NSF grant DMR-0101808.

References

- [1] Mitkova M 2000 *Insulating and Semiconducting Glasses* ed P Boolchand (Singapore: World Scientific) p 813
Also see
Fritzche H 2000 *Insulating and Semiconducting Glasses* ed P Boolchand (Singapore: World Scientific) p 653
- [2] Borisova Z U, Rivkova T S, Turkina T S and Tabolin A R 1984 *Russ. J. Inorg. Mat.* **20** 1796
For more recent work see
Bychkov E, Bychkov A, Pradel A and Ribes M 1998 *Solid State Ion.* **113–115** 691
- [3] Kawaguchi T, Maruno S and Elliott S R 1996 *J. Appl. Phys.* **79** 9096
- [4] Dejus R J, Susman S, Volin K J, Montague D G and Price D L 1992 *J. Non-Cryst. Solids* **143** 162
- [5] Dejus R J, LePoire D J, Susman S, Volin K J and Price D L 1991 *Phys. Rev. B* **44** 11705
- [6] Kawamoto Y, Nagura N and Tsuchihashi S 1973 *J. Am. Ceram. Soc.* **56** 289
- [7] Gutenev M, Tabolin A and Rykova A 1991 *Fiz. Khim. Stekla* **17** 36 (in Russian)

- [8] Iyetomi H, Vashishta P and Kalia R K 2000 *J. Non-Cryst. Solids* **262** 135
- [9] Massobrio C, Pasquarello A and Car R 2001 *Phys. Rev. B* **64** 144205
- [10] Cobb M and Drabold D A 1997 *Phys. Rev. B* **56** 3054
- [11] Penfold I T and Salmon P S 1991 *Phys. Rev. Lett.* **67** 97
- [12] Petri I, Salmon P S and Fischer H E 2000 *Phys. Rev. Lett.* **84** 2413
- [13] Eckert H 2000 *Insulating and Semiconducting Glasses* ed P Boolchand (Singapore: World Scientific) p 283
- [14] Boolchand P 2000 *Insulating and Semiconducting Glasses* ed P Boolchand (Singapore: World Scientific) p 191
- [15] Murase K 2000 *Insulating and Semiconducting Glasses* ed P Boolchand (Singapore: World Scientific) p 415
- Also see
- Cappelletti R 2000 *Insulating and Semiconducting Glasses* ed P Boolchand (Singapore: World Scientific) p 329
- [16] Micoulaut M 1998 *Eur. J. Phys. B* **1** 277
- [17] Kerner R and Phillips J C 2001 *Solid State Commun.* **117** 47
- [18] Georgiev D G, Boolchand P and Micoulaut M 2000 *Phys. Rev B* **62** R9228
- [19] Mitkova M, Wang Y and Boolchand P 1999 *Phys. Rev. Lett.* **83** 3848
- [20] Phillips J C 1979 *J. Non-Cryst. Solids* **34** 153
- [21] Thorpe M F, Jacobs D J, Chubynsky M V and Phillips J C 2000 *J. Non-Cryst. Solids* **266–269** 872
- [22] Zhang M and Boolchand P 1994 *Science* **266** 1355
- [23] Boolchand P and Bresser W J 2000 *Phil. Mag. B* **80** 1757
- [24] Carre D, Ollitrault-Fichet R and Flahaut J 1980 *Acta Crystallogr. B* **36** 245
- [25] Boolchand P and Bresser W J 2001 *Nature* **410** 1070
- [26] Rau C, Armand P, Pradel A, Varsamis C P E, Kamitsos E I, Granier D, Ibanez A and Philippot E *Phys. Rev. B* **63** 184204
- [27] Urena A, Fontana M, Arcondo B, Clavaguera-Mora M T and Clavaguera N 2002 *J. Non-Cryst. Solids* **304** 306
- [28] Boolchand P, Georgiev D G and Goodman B 2001 *J. Optoelectron. Adv. Mater.* **3** 703
- [29] Boolchand P, Feng X and Bresser W J 2001 *J. Non-Cryst. Solids* **293–295** 348
- [30] Phillips J C 2002 *Phys. Rev. Lett.* **88** 216401
- [31] Barnes A C, Lague S B, Salmon P S and Fischer H E 1997 *J. Phys.: Condens. Matter* **9** 6159
- [32] Kobayashi M 1990 *Solid State Ion.* **39** 121
- [33] Boolchand P, Georgiev D G, Qu Tao, Wang Fei, Cai Liuchun and Chakravarty S 2002 *C. R. Acad. Sci., Paris* at press
- [34] Penfold I T and Salmon P S 1990 *Phys. Rev. Lett.* **64** 2164
- [35] Wang Y, Wells J, Georgiev D G, Boolchand P, Jackson K and Micoulaut M 2001 *Phys. Rev. Lett.* **87** 185503